

Detailed study of the gain of the MWPCs for the LHCb muon system

E. Dané^a, G. Penso^{b,*}, D. Pinci^b, A. Sarti^a

^aINFN, Laboratori Nazionali di Frascati, Frascati, Italy

^bUniversità “La Sapienza” and INFN, Roma, Italy

Received 16 November 2006; received in revised form 19 December 2006; accepted 19 December 2006

Available online 31 December 2006

Abstract

The gain of a multiwire proportional chamber (MWPC) of the LHCb muon detector was measured precisely. The chamber, filled with a CO₂/Ar/CF₄ gas mixture, 55/40/5% in volume, was irradiated with a 1.3 GBq ¹³⁷Cs radioactive source and the current drawn by the chamber was measured. By precisely determining the primary ionization current it was possible to evaluate the absolute gain of the chamber. The dependence of the gain on the anode voltage and the gas density was measured and the need for a gain control system during the LHCb data taking is considered. Our experimental results are compared with those predicted for the chamber gain by Diethorn formula.

© 2007 Elsevier B.V. All rights reserved.

PACS: 29.40.Cs; 29.40.Gx; 29.90.+r

Keywords: Multiwire proportional chambers; Tracking and position-sensitive detectors; Elementary-particle and nuclear physics experimental methods and instrumentation

1. Introduction

The muon detector of the LHCb experiment [1] that will operate at the Large Hadron Collider (LHC) at CERN, consists of five muon tracking stations placed along the beam axis. The first station (M1), placed in front of the electromagnetic and hadronic calorimeters is composed of 24 triple-GEM [2,3] and 264 multiwire proportional chambers (MWPCs) [4,5]. The remaining four stations (M2–M5) comprise 1104 MWPCs and are placed downstream of the calorimeters. Each station is divided into four regions (R1–R4) [1], according to their distance from the beam axis. Each MWPC comprises two gas-gaps in station M1 and four gas-gaps in stations M2–M5. In all MWPCs the anode wire planes are centred in a 5 mm gap and consist [6] of 30 μm diameter gold-plated tungsten wires¹ with 2 mm spacing.

In the present paper we report a systematic study of the performance of a four-gap chamber belonging to the R3

region of station M3. As the geometry of the anode and cathode planes is identical for all MWPCs (two-gap and four-gap), the results presented in the following are valid for all the chambers of the muon detector.

2. Experimental setup

The set-up for chamber gain measurements consists (Fig. 1) of a steady table which supports the chamber to be tested and a 1.3 GBq ¹³⁷Cs source, screened by a lead case, which can be moved by an automated mechanical system [7] over the whole surface of the table. The dimension of the chamber is ~151 × 31 cm², the wires being parallel to the shorter side. One cathode plane is grounded in each gap. The opposite cathode plane is segmented in 24 pads: 12 of these are grounded and 12 are readout by a picoammeter (Fig. 2). The chamber is flushed (~50 cm³/min) with a CO₂/Ar/CF₄ gas mixture, 55/40/5% in volume.² The source is collimated and emits photons downwards. When the source is positioned on the chamber

*Corresponding author. Tel.: +390649914344.

E-mail address: gianni.penso@roma1.infn.it (G. Penso).

¹LUMA-METALL AB, Kalmar, Sweden.

²The same gas composition will be used during runs at the LHC.

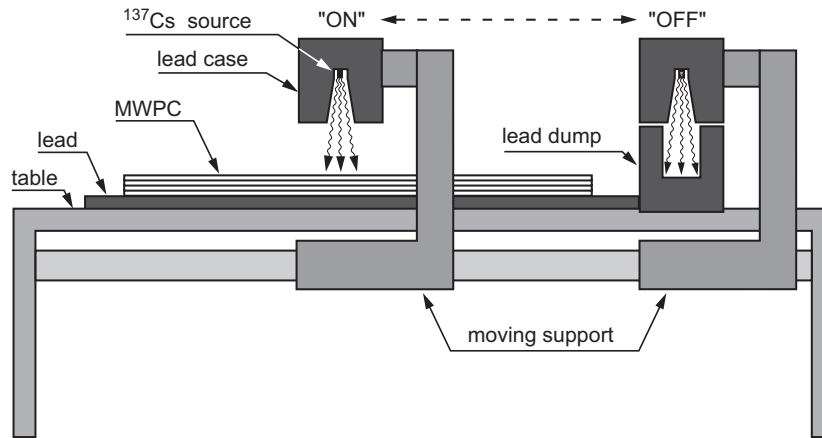


Fig. 1. Schematic view (not in scale) of the experimental setup. The ^{137}Cs source can be moved by an automated system over the table surface. The chamber current is measured with the source in the “ON” and “OFF” positions. The difference between these two values is the current due to source ionization.

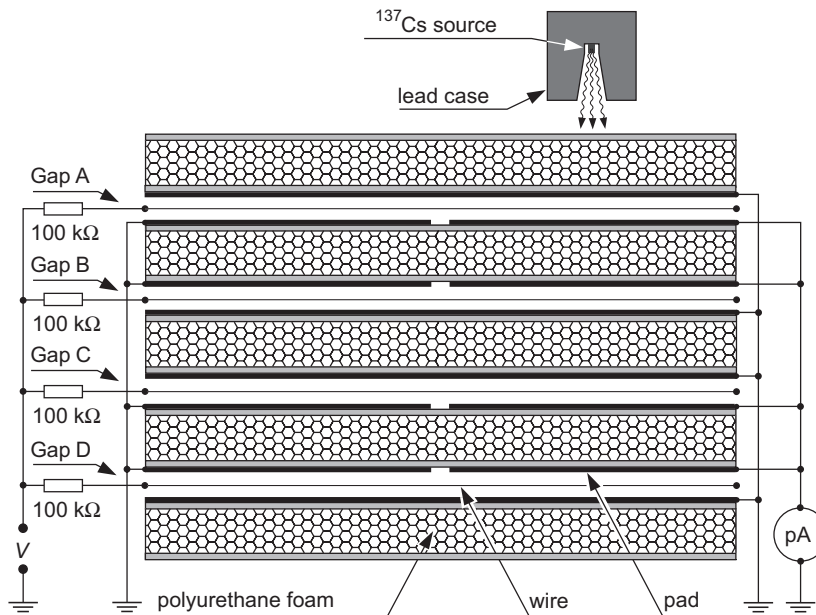


Fig. 2. Schematic cross-section (not in scale) of the chamber. The source in the “ON” position, the connections of the voltage supply (V) and of the picoammeter (pA) are shown.

(position “ON” in Figs. 1 and 2) the area of the chamber illuminated by the source is circular and has a diameter of about 10 cm. A 5 cm thick lead layer is placed under the chamber for radioprotection. The thickness of the chamber plates and the albedo from the lead layer are such that the ionization is equal in the four gaps within a few percent. The current (i) drawn by the chamber is read by a Keithley³ 6485 picoammeter connected to the non-grounded pads of the four gaps (Fig. 2). For a “zero-ionization” measurement the source is moved off the chamber to a “parking place” (position “OFF”, Fig. 1) where a lead dump absorbs the photons emitted by the source.

3. Measurements and results

3.1. Gain dependence on the anode voltage

The chamber current (i) measured with the source in the “ON” and “OFF” positions may fluctuate significantly because of the presence of eddy currents. Therefore, for each V value, this current is measured several tens times and averaged first in the “ON” position and immediately afterwards in the “OFF” position. As an example, we report in Fig. 3, for six different anode voltages V , a series of measurements of the current i in the “ON” and “OFF” source positions. The full process is automated and lasts a few minutes for each value of V . The difference between the

³Keithley Instruments Inc., Cleveland, OH, US.

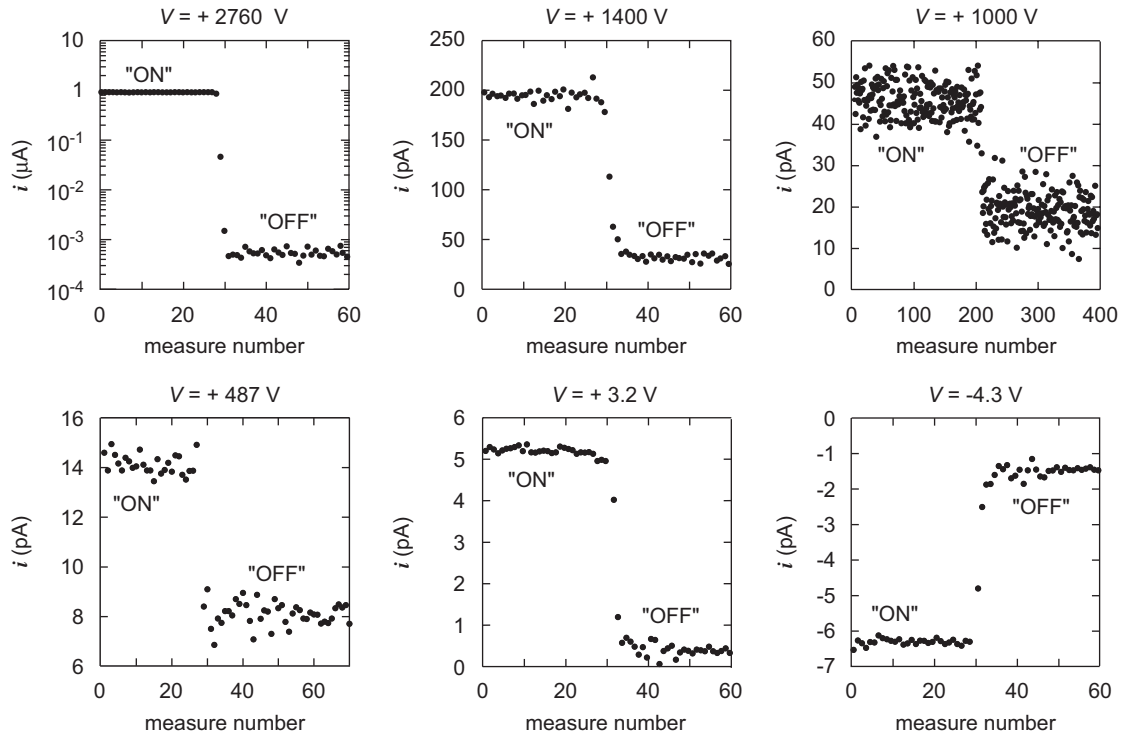


Fig. 3. Typical result of a series of current measurements. The six figures refer to different values of the wire voltage V . In each figure the first half of the points is measured with the source in the “ON” position. Then, without interrupting the measurement, the source is moved to the “OFF” position and the second half of the points is obtained.

average current measured with the source in the “ON” and “OFF” positions represents the chamber current $I(V)$ due to the radioactive source. The measurements were performed in the voltage range $-1 \leq V \leq 2.76$ kV. For $|V| \geq 500$ V the power supply was a CAEN⁴ model SY2527 mounted on a rack and connected to the chamber through a ~ 5 m-long high voltage cable. With this experimental setup the fluctuations in the measured current increase in percentage as the voltage V is decreased (upper charts in Fig. 3) and become comparable to the current itself at $V \approx 500$ V. At voltage $|V| < 500$ V the CAEN power supply was replaced by a variable number of 9 and 1.5 V standard alkaline batteries connected in series and placed close to the chamber. With this experimental setup the fluctuations in the measured current were drastically reduced (lower charts in Fig. 3) so that the current due to primary ionization could be measured easily (Fig. 4). As a check, this current was also measured with a reversed polarity of the wires (last chart in Fig. 3). In the latter case the electrons of the primary ionization are collected by the cathodes so that no multiplication occurs in the chamber and the current is independent of the voltage V as shown in Fig. 4. From these measurements we deduce that the current due to primary ionization is $I^* = 4.76 \pm 0.03$ pA. The gain $G(V)$ of the MWPC at a given wire voltage (V) is therefore given by

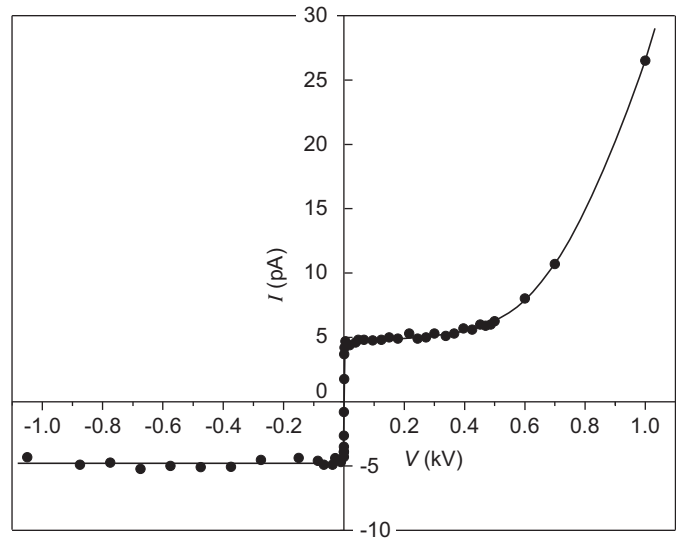


Fig. 4. Chamber current measured at an anode voltage $-1 \leq V \leq 1$ kV. For negative voltage and for low positive voltage only the primary ionization is collected, while at higher positive voltage the charge multiplication is observed. The line is drawn to guide the eye.

$G(V) = I(V)/I^*$. In Fig. 5 the chamber gain is reported as a function of the voltage V . In the nominal working region [7] of the chamber the gain ranges from $\sim 4.5 \times 10^4$ to $\sim 13.5 \times 10^4$.

⁴CAEN, 55049 Viareggio (LU), Italy.

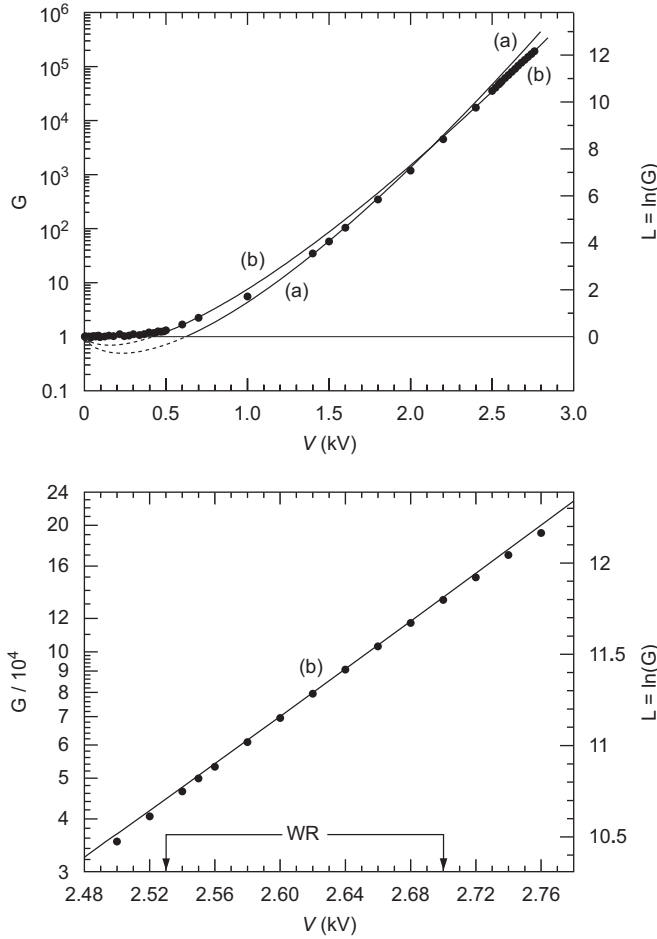


Fig. 5. Chamber gain as a function of the anode wires voltage V . Lines (a) and (b) are the predictions of the Diethorn formula for two different sets of the parameters E_{\min} and ΔV (see text). An expanded view of the high-voltage region is shown in the lower chart. The nominal working region (WR) of the chamber ($2.53 \leq V \leq 2.7$ kV) is shown.

3.2. Gain dependence on the gas density

In a MWPC the primary ionization current (I^*) and the gain (G) both depend on the gas density ρ . Therefore the current (I) drawn by the chamber also depends on ρ

$$I(\rho) = I^*(\rho) \times G(\rho). \quad (1)$$

Assuming the gas to behave like an ideal gas, ρ is proportional to the ratio P/T of its pressure (P) and its temperature (T). Starting from the normal⁵ gas pressure (P_0) and temperature (T_0), small variations $\Delta P \ll P_0$ and $\Delta T \ll T_0$ lead to a variation $\Delta\rho$ in the gas density given by

$$\frac{\Delta\rho}{\rho_0} = \frac{\Delta P}{P_0} - \frac{\Delta T}{T_0} \quad (2)$$

where ρ_0 is the gas density in normal conditions and $\Delta\rho \ll \rho_0$.

⁵In normal conditions the gas pressure P_0 and temperature T_0 are, respectively, the average atmospheric pressure and room temperature.

For a small deviation from the normal gas condition the gain variation ΔG is given by

$$\frac{\Delta G}{G_0} = \alpha \frac{\Delta\rho}{\rho_0} = \alpha \left(\frac{\Delta P}{P_0} - \frac{\Delta T}{T_0} \right) \quad (3)$$

where G_0 is the gain at normal pressure and temperature and α is a coefficient independent of P and T .

To determine the dependence of the primary ionization current (I^*) on the gas density we must distinguish two cases:

(i) the primary ionization is due to high-energy particles crossing the full gas gap, as will be the case in the LHCb experiment; in this case $\Delta I^*/I_0^* = \Delta\rho/\rho_0$ where ΔI^* is the variation in I^* corresponding to a variation $\Delta\rho$ in the gas density and $I_0^* = I^*(\rho_0)$.

(ii) the primary ionization is derived, as in the present test, from a radioactive gamma source. In this case the low-energy secondary electrons generated in the chamber may stop in the gas so that $\Delta I^*/I_0^* < \Delta\rho/\rho_0$. The two cases can be summarized by the formula

$$\frac{\Delta I^*}{I_0^*} = \beta \frac{\Delta\rho}{\rho_0} = \beta \left(\frac{\Delta P}{P_0} - \frac{\Delta T}{T_0} \right) \quad (4)$$

with $\beta = 1$ for high-energy crossing particles and $\beta < 1$ for a test with a radioactive source.

Taking into account Eqs. (1), (3) and (4), the variation ΔI in the chamber current due to small variations ΔP and ΔT in the gas pressure and temperature is given by

$$\frac{\Delta I}{I_0} = (\alpha + \beta) \left(\frac{\Delta P}{P_0} - \frac{\Delta T}{T_0} \right) \quad (5)$$

where $I_0 = I(\rho_0)$.

To determine the two coefficients α and β two series of measurements were performed. In the first series the dependence of the current I on ΔP was measured in the interval $0 \leq \Delta P \leq 20$ mbar. In the second series of measurements the variation ΔI^* in the primary ionization current corresponding to a variation of $\Delta P = 20$ mbar was determined. In all these measurements the temperature was kept constant so that Eqs. (3)–(5) become

$$\frac{\Delta G}{G_0} = \alpha \frac{\Delta P}{P_0} \quad (6)$$

$$\frac{\Delta I^*}{I_0^*} = \beta \frac{\Delta P}{P_0} \quad (7)$$

$$\frac{\Delta I}{I_0} = (\alpha + \beta) \frac{\Delta P}{P_0}. \quad (8)$$

To perform the first series of measurements the pressure inside (but not outside) the chamber was increased from its initial value of P_0 to a final value of $P_0 + 20$ mbar. This internal overpressure ΔP causes an undesired deformation of the two external cathode panels⁶ of gaps A and D (see insert in Fig. 6) so that the width of these gaps becomes

⁶With an overpressure of 20 mbar this deformation is about 150 μm at the centre of the chamber.

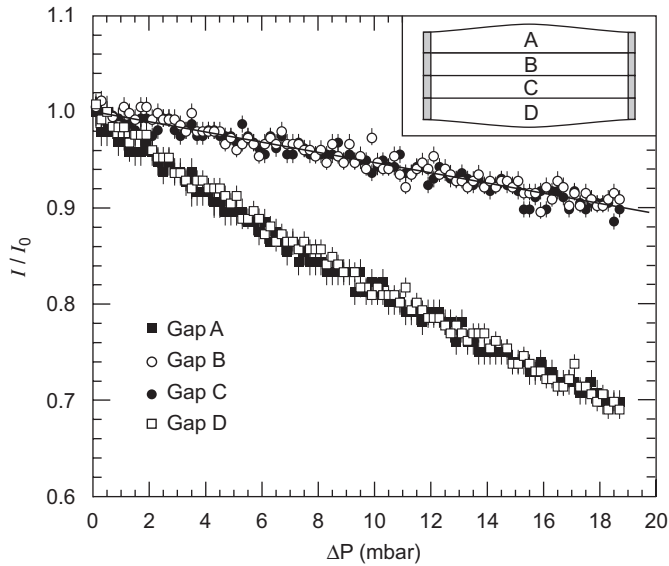


Fig. 6. Measured current of the four gaps as a function of the overpressure ΔP of the gas inside the chamber. The currents are normalized to their values at $\Delta P = 0$. The overpressure ΔP causes a slight deformation of the external panels of the chamber (see insert) which is responsible for the lower gain observed for gaps A and D. During the data-taking at the LHC, the pressure inside and outside the chamber will be the same, so that all the gaps will behave like the gaps B and C. The data reported here refer to an anode voltage of 2750 V but similar results are obtained in the interval $2500 \leq V \leq 2750$ V. The line is a linear fit to the data relative to gaps B and C.

larger than their normal value and their gain is lowered. This effect is not present in gaps B and C because there is no pressure difference between these and the neighbouring gaps. For these reasons the currents I_A , I_B , I_C and I_D of the four gaps were measured separately as a function of the overpressure ΔP , but only the data relative to gaps B and C were used to determine the effect of a pressure variation on the response of a normal (not inflated) chamber. In Fig. 6 we report, as a function of ΔP , the measured currents of the four gaps I_A , I_B , I_C and I_D normalized to their respective values ($I_0^A, I_0^B, I_0^C, I_0^D$) at $\Delta P = 0$. These data were taken at a voltage $V = 2750$ V with the source in the “ON” position. The current with the source in the “OFF” position was not measured because at high voltage ($V \geq 2500$ V) this current is negligible compared with the current in the “ON” position (see chart 1 in Fig. 3). As expected, the currents in the inflated gaps A and D (Fig. 6) are lower than those measured for gaps B and C and cannot be used for our purposes. A linear fit to the data relative to gaps B and C leads to the relation:

$$I_{B,C}/I_0^{B,C} = 1 - (5.1 \pm 0.2) \times 10^{-3} (\text{mbar}^{-1}) \Delta P. \quad (9)$$

Taking into account Eq. (8) we deduce⁷ $\alpha + \beta = -5.0 \pm 0.2$. This measurement, repeated for different values of the

⁷During the measurements the atmospheric pressure was $P_0 \approx 990$ mbar.

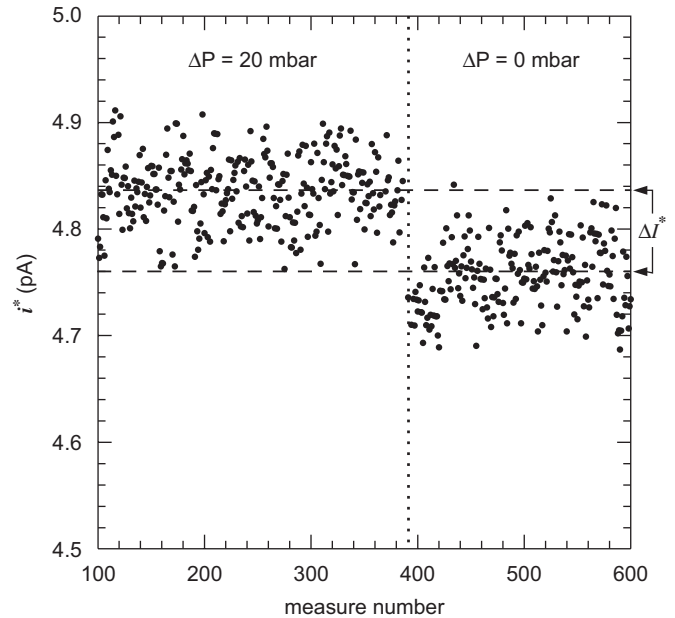


Fig. 7. Measurement of the primary ionization current at two different gas overpressures. During the first 390 measurements the gas overpressure inside the chamber was $\Delta P = 20$ mbar. This overpressure was then removed and the last 210 measurements were taken. The horizontal dashed lines represent the average ionization current at $\Delta P = 20$ mbar and at $\Delta P = 0$ mbar.

anode voltage V in the interval 2.5–2.75 kV, leads within the errors, to the same value of $\alpha + \beta$.

In the second series of measurements the anode voltage was set to 47 V and the primary ionization current i^* of the chamber was measured at $\Delta P = 20$ mbar and at $\Delta P = 0$, with the source in the “ON” position. Because no charge multiplication occurs at this voltage, the chamber deformation described above has no effect on the measured current. Due to large current fluctuations the current i^* was measured several hundred times (Fig. 7) and then averaged. The difference⁸ between the average current (I^*) at $\Delta P = 20$ mbar and at $\Delta P = 0$ was found to be (Fig. 7) $\Delta I^* = 0.078 \pm 0.002$ pA. Taking into account Eq. (7) where I_0^* has already been measured at 4.76 ± 0.03 pA, we deduce $\beta = 0.81 \pm 0.03$. From the results of the two series of measurements we deduce $\alpha = -5.8 \pm 0.2$ for an anode voltage in the range 2.5–2.75 kV, which includes the nominal working region [7] of the chamber $2.53 \leq V \leq 2.7$ kV.

In the LHCb experiment the gas pressure in the muon chambers will be kept at atmospheric pressure to avoid any deformation of the chamber. The meteorological data⁹ reported in Fig. 8 show that over a period of 10 years $\Delta P/P_0$ can reach $\pm 3.1\%$. Taking into account Eq. (8), this variation in the atmospheric pressure will result in a

⁸The current i^* was not measured in the “OFF” source position because its value would be canceled out in the average current subtraction.

⁹These data, provided by the “Office Fédéral de Météorologie et Climatologie MétéoSuisse”, refer to the Geneva area.

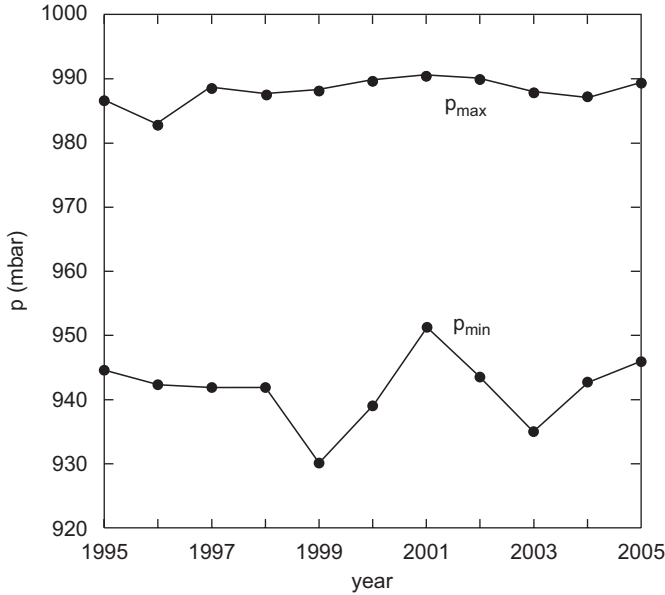


Fig. 8. Absolute annual maximum and minimum atmospheric pressure in Geneva. The data refer to the years 1995–2005.

variation in the response of the chambers¹⁰ of about $\pm 15\%$ which corresponds to a variation in the anode high-voltage of about ± 23 V. The effect of temperature variation on the chamber response should also be present, as predicted by Eq. (3). Nevertheless, because the LHCb apparatus is located about 100 m underground, the temperature variation ($\Delta T/T_0$) is expected to be much smaller than the variation ($\Delta P/P_0$) in atmospheric pressure. Because the overall effect of pressure and temperature variations is not negligible, a control system is envisaged to stabilize the response of the chambers.

4. Comparison of the experimental results with the Diethorn formula

The dependence of the gain G on the voltage V and on the gas density ρ is often described by the Diethorn formula [8], which assumes that the first Townsend coefficient is proportional to the electric field. According to that formula the function $G(V)$ is given by:

$$G(V, \rho) = \left(\frac{V}{A(\rho)} \right)^{(V/B)} \quad (10)$$

where:

$$A(\rho) = r_a \ln(r_c/r_a) E_{\min} \frac{\rho}{\rho_0} \quad (11)$$

$$B = \frac{\ln(r_c/r_a) \Delta V}{\ln 2} \quad (11')$$

¹⁰During the experiment the particles will cross the full gas gap so that $\beta = 1$ and in Eq. (8) $\alpha + \beta \simeq -4.8$.

and where r_a is the radius of the anode wires, r_c is the “equivalent cathode radius” [9,10], E_{\min} is the minimum electric field needed to start the avalanche at the normal gas density ρ_0 and ΔV (multiplied by the electron charge) is the average energy required to produce one more electron in the avalanche [11]. For all the LHCb muon chambers, $r_a = 15 \mu\text{m}$ and $r_c \simeq 16.2 \text{mm}$. At normal gas density ($\rho = \rho_0$) the two parameters E_{\min} and ΔV fully determine the function $L(V)$ and its derivative $D(V)$:

$$L(V) \equiv \ln[G(V, \rho_0)] = \frac{V}{B} \ln \left(\frac{V}{A(\rho_0)} \right) \quad (12)$$

$$D(V) \equiv \frac{dL}{dV} = \frac{1}{B} \left(1 + \frac{BL(V)}{V} \right). \quad (13)$$

From Eqs. (11)–(13) we obtain

$$E_{\min} = \frac{V \exp[L(V)/(L(V) - VD(V))]}{r_a \ln(r_c/r_a)}. \quad (14)$$

$$\Delta V = \frac{V \ln 2}{(VD(V) - L(V)) \ln(r_c/r_a)}. \quad (14')$$

The two quantities E_{\min} and ΔV are proper to the gas, so that expressions (14) and (14') should be independent of V in the voltage interval where the Diethorn formula is valid. To determine E_{\min} and ΔV from Eqs. (14) and (14') we used the 26 points (Fig. 5) measured¹¹ at $V_i \geq 500$ V ($i = 1, 26$). While $L(V_i)$ were obtained directly from the data, $D(V_i)$ have been calculated as the derivative of a second order polynomial passing through the considered i -th point $L(V_i)$ and the two neighbouring points $L(V_{i-1})$ and $L(V_{i+1})$. The result of these calculations, reported in Fig. 9, shows that in the interval $1.6 \leq V \leq 2.4$ kV E_{\min} and ΔV are practically independent of V and given by $E_{\min} = 60 \pm 2$ kV/cm and $\Delta V = 32 \pm 1$ V. The Diethorn formula is therefore valid in the interval $1.6 \leq V \leq 2.4$ kV and the above values of E_{\min} and ΔV are characteristic of the gas mixture used. In Fig. 5 (curve a) we show the function $G(V)$ calculated according to Eqs. (10) (11) and (11') and assuming $E_{\min} = 60$ kV/cm and $\Delta V = 32$ V. As expected, this curve fits well the experimental points in the region $1.6 \leq V \leq 2.4$ kV.

At voltages outside the interval $1.6 \leq V \leq 2.4$ kV Diethorn formula still can be used to describe the experimental behaviour of $G(V)$. But in that case E_{\min} and ΔV are two parameters of the formula with no relation to the gas characteristics. For example, at the central value $V = 2615$ V of the nominal working region [7] of the chamber, we have (Fig. 9) $E_{\min} \simeq 41$ kV/cm and $\Delta V \simeq 42$ V. The prediction of the Diethorn formula, calculated with these two parameter values, is shown in Fig. 5 (curve b). As expected, the agreement with the experimental points is good only in the working region of the chamber.

¹¹At a voltage below ≈ 500 V Diethorn formula gives a gain $\lesssim 1$ and is therefore out of its range of validity.

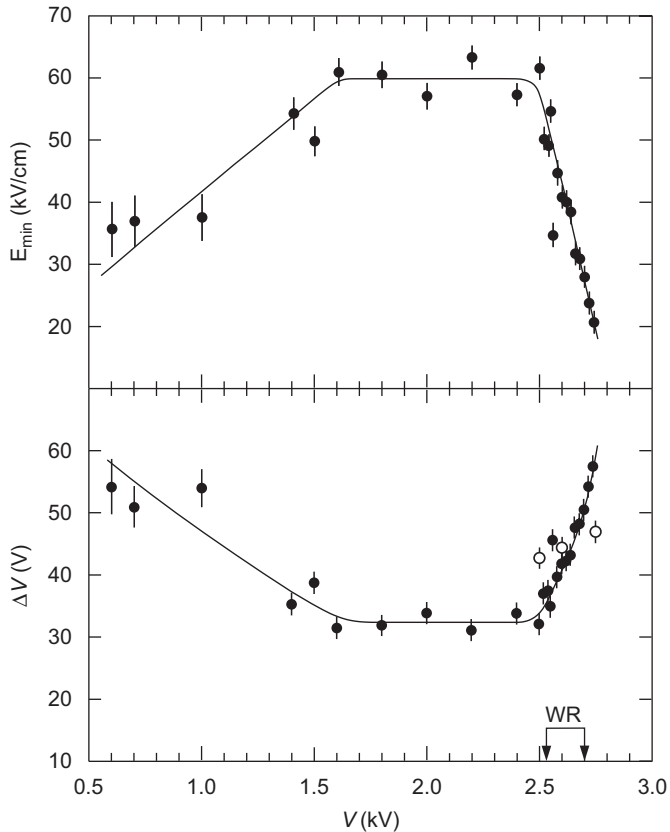


Fig. 9. Full points: Values of the two Diethorn parameters E_{\min} and ΔV as a function of anode voltage V , calculated from the measured gain dependence on V . E_{\min} and ΔV are independent of V in the region $1.6 \leq V \leq 2.4$ kV which corresponds to the range of validity of the Diethorn formula (see text). The open points represent the value of ΔV obtained from the measured gain dependence on gas pressure. The nominal working region (WR) of the chambers [7] is shown on the V axis. The curves are drawn to guide the eye.

The experimental dependence of the chamber gain on the gas pressure [12,13] can also be compared with the prediction of Diethorn formula. From Eqs. (6), (10), (11) and (11') one can easily deduce the relations $\alpha = -V/B$ and $\Delta V = -V \ln 2/\alpha \ln(r_c/r_a)$. Taking into account the experimental value of $\alpha = -5.8 \pm 0.5$ obtained in the voltage interval 2.5–2.75 kV, we deduce a value of ΔV of 44 ± 3 V in agreement with the value of 42 ± 2 V obtained by fitting the $G(V)$ data in the voltage interval $2.53 \leq V \leq 2.7$ kV.

5. Conclusions

The gain of a typical muon chamber of the LHCb experiment was measured with high precision as a function of the anode voltage. The chamber was filled with a $\text{CO}_2/\text{Ar}/\text{CF}_4$ gas mixture, 55/40/5% in volume. In the interval $1.6 \leq V \leq 2.4$ kV the Diethorn formula is found to be valid and to fit well the experimental gain values $G(V)$. The two parameters E_{\min} and ΔV , which are proper to the gas mixture, were determined to be $E_{\min} = 60 \pm 2$ kV/cm and $\Delta V = 32 \pm 1$ V.

The dependence of the chamber gain on the gas pressure was also measured in the working region of the chambers $2.53 \leq V \leq 2.7$ kV and a variation of $\simeq 0.5\%$ per mbar is expected when the experiment will run at the LHC. During long-term operation the changes of atmospheric pressure can result in a variation of about $\pm 15\%$ in the response of the chambers which corresponds to a variation in the anode high-voltage of about ± 23 V. This effect being non-negligible, a chamber-response control system is foreseen during the data-taking period.

References

- [1] LHCb Collaboration, LHCb Muon System Technical Design Report, CERN/LHCC 2001-010 (2001), and Addendum to the Muon System Technical Design Report, CERN/LHCC 2003-002 (2003).
- [2] G. Bencivenni, et al., Nucl. Instr. and Meth. A 513 (2003) 264.
- [3] M. Alfonsi, et al., IEEE Trans. Nucl. Sci. NS-51 (2004) 2135.
- [4] M. Anelli et al., LHCb Note CERN-LHCb-2005-003 (2005).
- [5] M. Anelli et al., LHCb Note CERN-LHCb-2005-079 (2005).
- [6] P. Ciambione, et al., Nucl. Instr. and Meth. A 545 (2005) 156.
- [7] M. Anelli, et al., IEEE Trans. Nucl. Sci. NS-53 (2006) 330.
- [8] W. Diethorn, A methane proportional counter system for natural radiocarbon measurement, Thesis, USAEC Report NY06628, 1956.
- [9] E. Mathieson, Induced Charge Distributions in Proportional Detectors, BNL note (1991), available: (<http://www.inst.bnl.gov/publications/Mathieson.shtml>).
- [10] W. Riegler, Detector Physics and Performance Simulations of the MWPCs for the LHCb Muon System, LHCb Note, CERN-LHCb-2000-060 (2000); id. version 2 (2003), available: (<http://indico.cern.ch/conferenceDisplay.py?confId=a03841>).
- [11] W. Blumm, L. Rolandi, in: F. Bonaudi, C.W. Fabjan (Eds.), Particle Detection with Drift Chambers, Springer, Berlin, 1994.
- [12] D. Pinci, A. Sarti, Study of the MWPC gas gain behaviour as a function of the gas pressure and temperature, LHCb Note, CERN-LHCb-2005-079, 2005.
- [13] E. Dané, D. Pinci, A. Sarti, Report on the quality of the LHCb-Muon four-gap MWPC produced at LNF, LHCb Note, CERN-LHCb-2006-053, 2006.